Fission of doubly ionized calcium clusters

Estela Blaisten-Barojas [a,*], Chang-Hong Chien [a], Mark R. Pederson [b], Jeff W. Mirick [a]

[a] *School of Computational Sciences, George Mason University, MSN 5C3, Fairfax, VA 22030, USA*
[b] *Center for Computational Materials Science, Naval Research Laboratory, Washington, DC 20375-5320, USA*

Abstract

Cluster ions, Ca_N^+ and Ca_N^{2+}, containing up to $N = 8$ atoms are studied within density functional theory. Ground and first excited states, and ionization energies are reported for all sizes. At zero temperature Ca_3^{2+} and Ca_4^{2+} are linear, whereas Ca_5^{2+} through Ca_7^{2+} undergo structural transitions from 3D-configurations into linear ions below 600 K. As a consequence, fission that occurs above 600 K starts from linear configurations. Ca_8^{2+} has an hexagonal bipyramidal structure. The preferred fission channels are $Ca_N^{2+} \rightarrow Ca^+ + Ca_{N-1}^+$ with fission barriers smaller than the evaporation energy up to Ca_7^{2+}. However, Ca_8^{2+} presents a large fission barrier and would rather evaporate one atom than undergo fission.
© 2004 Elsevier B.V. All rights reserved.

1. Introduction

Laser ionization techniques and mass spectrometry have allowed the experimental observation of multiply ionized clusters [1–3]. Not all sizes of these cluster ions are stable, and the smallest size observed experimentally is known as the *appearance size*. Clusters below this size lose charge and mass by fragmentation along various channels. This appearance size depends on the material. For example, for doubly ionized alkali metal clusters, the appearance size is large: 27 for Na, 20 for K, 24 for Rb, and 23 for Cs [2–4]. In contrast, the doubly ionized alkaline earth clusters present small appearance sizes: 6 for Mg, 8 for Ca and Sr, and 7 for Ba [5–7]. This fragmentation process is driven by Coulomb repulsive forces and carries the name of *fission*.

The name *fission* is borrowed from the nuclear physics depiction of the atomic nucleus splitting into two or more parts. In multiply ionized clusters it is used to describe the Coulomb-induced fragmentation. As in nuclear reactions, depending upon the forces involved, the fission of a cluster gives rise to two charged cluster-

fragments, or proceeds through multi-fragment processes. A nuclear fission reaction is initiated by bombarding fissionable nuclei with neutrons. A cluster fission reaction is possible when the internal energy of the multiply ionized cluster is larger than a fission energy barrier. It is commonly believed that no fission occurs when this fission barrier is larger than the energy needed to evaporate a neutral atom. Both the evaporation energy and the fission barrier are intimately related to the bonding energy in the cluster. For this reason, attempts to formulate a general description of the fragmentation mechanism for different elements is highly speculative [8,9].

In this work, we study the fragmentation of doubly ionized clusters up to Ca_8^{2+} and predict the fission barriers and evaporation energies involved in the process. We confirm that Ca_8^{2+} is the appearance size for fission [5] and predict that this is a thermally stable ion.

2. Structure of neutral, singly and doubly ionized calcium clusters

The generalized gradient approximation (GGA) and a 19-gaussians basis set optimized for the spin unpolarized

---

* Corresponding author. Fax: +703 993 1993.
E-mail address: blaisten@gmu.edu (E. Blaisten-Barojas).

Ca atom [10] are used throughout. The basis set was contracted 7s5p3d to which three floating gaussians were added. Calculation of the first three ionization potentials of atomic Ca gives 6.07, 11.994, and 50.909 eV, which compare very well to the experimental data of 6.113, 11.872, and 50.913 eV, respectively. These are all-electron calculations performed without symmetry constraints using the NRLMOL package [11].

The ground state of neutral stable clusters, and the ground and first excited state of singly and doubly ionized clusters up to $N = 8$ were calculated and are reported in Table 1, columns 3–7. Dashed-filled spaces in this table indicate that the structure was not stable, and bold type characters identify the most stable structure in the ground state. Ground states of Ca_N^+ are doublets (the multiplicity is given as upper left index). Ground states of Ca_N^{2+} are singlets (upper left index). The excited states are quartets for Ca_N^+ and triplets for Ca_N^{2+} with the exception of the distorted pentagonal bipyramid Ca_7^{2+} where singlet and triplet states are almost degenerate (both energies in bold type). Reported binding energies of the neutral clusters, E_N, are referred to energies of separated atoms. Cluster ions binding energies are defined as: $E_N^+ = -E_{total}(Ca_N^+) + (N-1)E_1 + E_1^+$ and $E_N^{2+} = -E_{total}(Ca_N^{2+}) + (N-2)E_1 + 2E_1^+$. Columns 8 and 9 in Table 1 list the first and second ionization potentials. Note that the ionization potentials of the linear clusters is lower than the corresponding 3D counterpart for all sizes.

Ca_2^{2+} is more tightly bound than both Ca_2 and Ca_2^+. Their vibrational frequencies are 154, 72 and 124 cm^{-1}, respectively. The dissociation of Ca_2^{2+} into two atomic Ca^+ is exothermic (negative sign in Table 1) and occurs by overcoming a 0.39 eV barrier at the inter-

atomic distance of 5.5 Å. The other sizes of singly ionized clusters are more tightly bound than their neutral counterparts [12]. Furthermore, the positive charge is distributed such as to stretch atoms as far apart as possible. Therefore, Ca_3^+, Ca_3^{2+}, and Ca_4^{2+} are linear cluster ions. Even though the lowest energy structures of Ca_5^{2+} (trigonal bipyramid) and Ca_6^{2+} (decorated trigonal bipyramid) are not linear, the second to lowest structures are linear with binding energies less than 0.1 eV above the global minimum as seen in Table 1. Ca_7^{2+} and Ca_8^{2+} global minimum structures are the pentagonal bipyramid and the hexagonal bipyramid. Almost all other three dimensional (3D) structures of the heptamer and octamer cluster ions are unstable. However, linear Ca_7^{2+} and Ca_8^{2+} are stable higher energy isomers. The bond lengths in all these cluster ions are slightly longer than in the neutral clusters measuring 3.6–4.0 Å.

As is clear from the data in Table 1, several structures are not stable in the excited state (quartet and triplet states of Ca_N^+ and Ca_N^{2+} are denoted with 4 and 3 left upper indices, respectively). $^4Ca_2^+$ and triangular $^3Ca_3^{2+}$ are bound, although they do not dissociate into neutral Ca and ionized Ca^+ in their ground states (negative sign in the table reflects the arbitrary origin of energies). Few ground state structures are preserved in the excited states and these are only 0.1–0.3 eV above the ground state. Therefore, it is not excluded that in the experiments [5–7] several detected cluster ions are in excited states.

The charge distribution of Ca_N^{2+} is non-uniform such that not all atoms are equivalent in a given cluster ion, as shown in Table 2. The charge distribution in Ca_N^+ is raughly the same as for Ca_N^{2+} with half of the charges. Linear cluster ions have the largest charge on the end

Table 1
Binding energy of neutral, singly and doubly ionized clusters and the first two ionization potentials in eV

	Geom	^1E_b	$^2E_b^+$	$^1E_b^{2+}$	$^4E_b^+$	$^3E_b^{2+}$	E_I	E_{II}
Ca₂		0.201	1.264	−1.869	−0.834	---	5.007	9.204
Ca₃	L	0.446	**2.045**	**0.235**	0.489	---	4.472	7.880
	TI	---	1.912	---	---	---		
	TE	**0.742**	---	---	1.148	−0.625		
Ca₄	L	0.705	**2.644**	**2.090**	1.350	---	4.130	7.058
	R	---	---	1.786	---	0.320		
	T	**1.779**	---	---	2.071	0.828		
Ca₅	L	0.970	3.150	2.737	2.025	1.852	3.890	6.483
	TB	**2.414**	**4.163**	**3.193**	3.168	2.178	4.322	7.041
Ca₆	L	1.243	3.605	4.062	2.595	2.781	3.709	6.046
	O	---	---	---	4.417	---		
	DTB	**3.122**	**4.892**	**4.181**	4.495	3.628	4.300	7.209
Ca₇	L	0.457	3.999	4.384	3.093	3.561	2.313	5.685
	PB	**4.228**	**5.906**	**4.857**	---	**4.900**	4.392	7.118
Ca₈	L	0.025	4.412	5.051	3.542	4.241	1.684	5.431
	HB	4.272	6.139	**6.429**	---	---		5.780
	DPB	**5.033**	**6.885**	---	6.559	6.053	4.217	
Ca₉	L			5.272		4.847		
	DDPB			7.522		7.378		

Upper left indices refer to the multiplicity of the electronic state. Geometries correspond to ground state, distortions occur in the ions. Dashes stand for unstable structures. Abbreviations: linear (L), isoceles triangle (TI), equilateral triangle (TE), rhombus (R), tetrahedron (T), trigonal bipyramid (TB), octahedron (O), decorated TB (DTB), pentagonal bipyramid (PB), hexagonal bipyramid (HB), decorated PB (DPB), doubly DPB (DDPB).

Table 2
Charge distribution of the stable calcium cluster ions

	Geometry	Charge summed to atoms (e)
Ca_3^{2+}	linear	0.8, 0.4, 0.8
Ca_4^{2+}	rhombus	long diagonal: 0.52, 0.52
		short diagonal: 0.48, 0.48
Ca_4^{2+}	linear	0.6, 0.4, 0.4, 0.6
Ca_5^{2+}	trigonal	apexes: 0.47, 0.47
	bipyramid	reminder: equally distributed on three atoms
Ca_5^{2+}	linear	0.53, 0.29, 0.37, 0.29, 0.53
Ca_6^{2+}	dec-trig	atoms on plane: 0.35, 0.46, 0.46, 0.35
	bipyramid	other: 0.19,0.19
Ca_6^{2+}	linear	0.46, 0.24, 0.3,0.3, 0.24, 0.46
Ca_7^{2+}	distorted	apexes: 0.23, 0.23
	pen. bipy.	on ring: 0.31, 0.26, 0.4, 0.26, 0.31
Ca_7^{2+}	linear	0.405, 0.2, 0.27, 0.25, 0.27, 0.2, 0.405
Ca_8^{2+}	linear	0.36, 0.18, 0.23, 0.22, 0.22, 0.23, 0.18, 0.36
Ca_8^{2+}	hexagonal	apexes: 0.2, 0.2
	bipyramid	reminder: equally distributed on six atoms

atoms. In the 3D cluster ions, the charge distribution keeps the same point symmetry as the cluster structure. For example, in Ca_8^{2+} the apexes of the bipyramid carry +0.2e each, and the reminding 1.6e is equally distributed on the 6-atom-hexagonal ring. In Ca_7^{2+} there is a distortion of the D_{5h} (pentagonal bipyramid) such that the two apex atoms carry +0.23e but the reminder charge is not equally distributed among the 5-atom-ring. The result is one longer bond in the ring between the two atoms carrying 0.31e each.

The above results are for zero temperature. On the other hand, experiments are performed at finite temperatures. Therefore, we investigated the possibility that 3D cluster ions become linear at finite temperatures. Indeed they do. By using the harmonic frequencies of the normal modes of the stable isomers, we calculated their free energy as a function of temperature. We predict that whereas linear Ca_4^+ through Ca_8^+ are not favored at temperatures below 600 K, Ca_5^{2+} through Ca_7^{2+} undergo structural transitions to linear clusters. The predicted transition temperatures are: 280, 350 and 540 K for Ca_5^{2+}, Ca_6^{2+}, and Ca_7^{2+}, respectively. The transition temperature of Ca_7^{2+} in the triplet state is 730 K. In this temperature range Ca_8^{2+} remains an hexagonal bipyramid.

3. Fragmentation channels for fission and evaporation

Using results in Table 1, we calculate the energy difference between initial and final states of all possible fragmentation channels of linear doubly ionized clusters (the *parents*) as

$$D_m^c(N) = E_N^2 - (E_{N-m}^{2-c} + E_m^c), \qquad (1)$$

where $c = 1$ is a fission channel, $c = 0$ is an evaporative channel, and m is the size of one of the two *daughter fragments*. Two fragmentation types are identifiable. In the fission process the fragmentation channels lead to

two singly charged fragments and $D_m^1(N)$ characterizes the final states. In the evaporation process the fragmentation channels lead to one neutral fragment and one doubly charged fragment characterized by $D_m^0(N)$. A special case of the evaporative channels is $D_1^0(N)$, the energy to evaporate one neutral atom from a doubly ionized N-atom cluster. This energy is referred as *evaporation energy*.

The energy balance $D_m^c(N)$ is shown in Fig. 1a as a function of parent size when parent and daughters are linear. Dashed lines refer to the evaporative channels where a neutral fragment is lost. The evaporation energy $D_1^0(N)$ (crosses/dashed line) clearly decreases as size increases. This decrease with size is expected, because as the doubly charged cluster becomes larger, the Coulomb repulsion per atom decreases. Full lines correspond to fission channels in which each fragment has a charge of one. Negative values along the fission channels indicate that the fragments are more stable than the fragmenting doubly charged parent ion. When this happens the fission channels are exothermic.

Fragmentation of these linear clusters along fission channels $Ca_N^{2+} \rightarrow Ca_{N-m}^+ + Ca_m^+$ occur when the system has enough energy to overcome an energy barrier V_m.

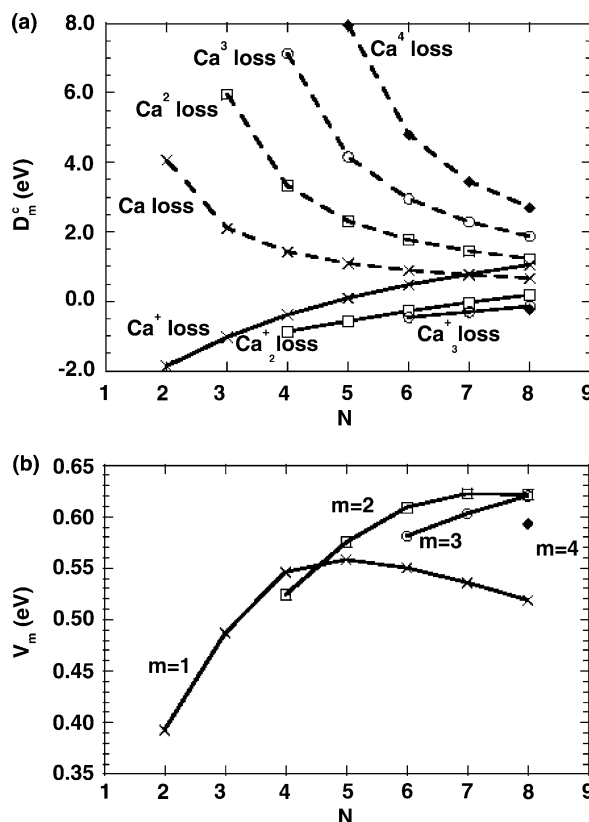
Fig. 1. Linear Ca_N^{2+} fragmenting into linear fragments. (a) Energy balance between initial and final states of evaporative channels with $c = 0$ (dotted lines) and of fission channels with $c = 1$ (full lines) with all possible mass losses: $m = 1$ (crosses), 2 (squares), 3 (circles), 4 (black dimond). (b) Energy barrier for the fission channels loosing linear fragments of mass $m = 1$ (crosses), 2 (squares), 3 (circles), 4 (dimond).

Calculation of this barrier is not trivial because the intermediate compound at the saddle point should be a singlet with paired spins whereas the singly charged fragments are doublets. Therefore, we prepared each fragment at infinity: one with its unpaired electron spin up, and the other with the unpaired spin down. By approaching from infinity, these two fragments form an activated compound that has truly paired spins (antiferromagnetic). This was absolutely necessary, otherwise the fragments at infinity would be in spin averaged states (paramagnetic) and would not lead to reliable values of the energy barrier. Results are illustrated in Fig. 1b that shows the energy barrier V_m corresponding to fission channels where one m-atom fragment (singly charged) is produced from a parent of size N. The other singly charged fragment in each channel has size $N - m$. The doubly charged linear clusters always fission because the barriers are lower than the evaporation energy. The reported barrier values are upper bounds to the true barriers, because the fragments were not relaxed along the fragmentation path. The relaxation energy is small though, since bonds relax at most 0.2 Å. Among the various fission channels, the fragmentation $Ca_N^{2+} \rightarrow Ca_{N-1}^+ + Ca^+$ is energetically preferred at all sizes except Ca_4^{2+} (two Ca_2^+ fragments) as shown in Fig. 1b.

Ca_8^{2+} is not linear at intermediate temperatures. For this 3D case the energy balance of the fragmentation process, Eq. (1), could still be used. However, the atoms are non-equivalently charged in the parent ion and one must make assumtions as to what geometries the fragments acquire in the final state. In Fig. 2, we depict the eight possible fragmentation patterns of Ca_8^{2+} in the hexagonal bipyramidal structure. There are two non-equivalent channels for each reaction: $Ca_8^{2+} \rightarrow Ca_7^+ + Ca_1^+, \rightarrow Ca_6^+ + Ca_2^+, \rightarrow Ca_5^+ + Ca_3^+,$ and $\rightarrow Ca_4^+ + Ca_4^+$.

To add to the complexity, the fragments shown in Fig. 2 might not be the final state, because either further fragmentation may occur, or the 3D structures are unstable. Therefore quantities such as Eq. (1) are not well defined for 3D ions. With this constraint in mind, we only determined the energy barrier leading to each of the eight fragmentation patterns shown in Fig. 2. The strategy to determine the energy barriers was the same used for the linear cluster ions. Namely, the unrelaxed fragments were prepared one with spin up and the other with spin down such that when approached they form an antiferromagnetic activated compound at the saddle point. Therefore the potential energy paths studied correspond to the approach of the centers of mass of two fragments without allowing for rotation. The energy barriers along these paths were calculated for all channels sketched in Fig. 2. The fission channel with the lowest energy barrier corresponds to Fig. 2a. The corresponding potential energy path is shown in Fig. 3 (circles). The relaxation energy of the pentagonal bipyramid fragment shown in Fig. 2a is small, therefore the
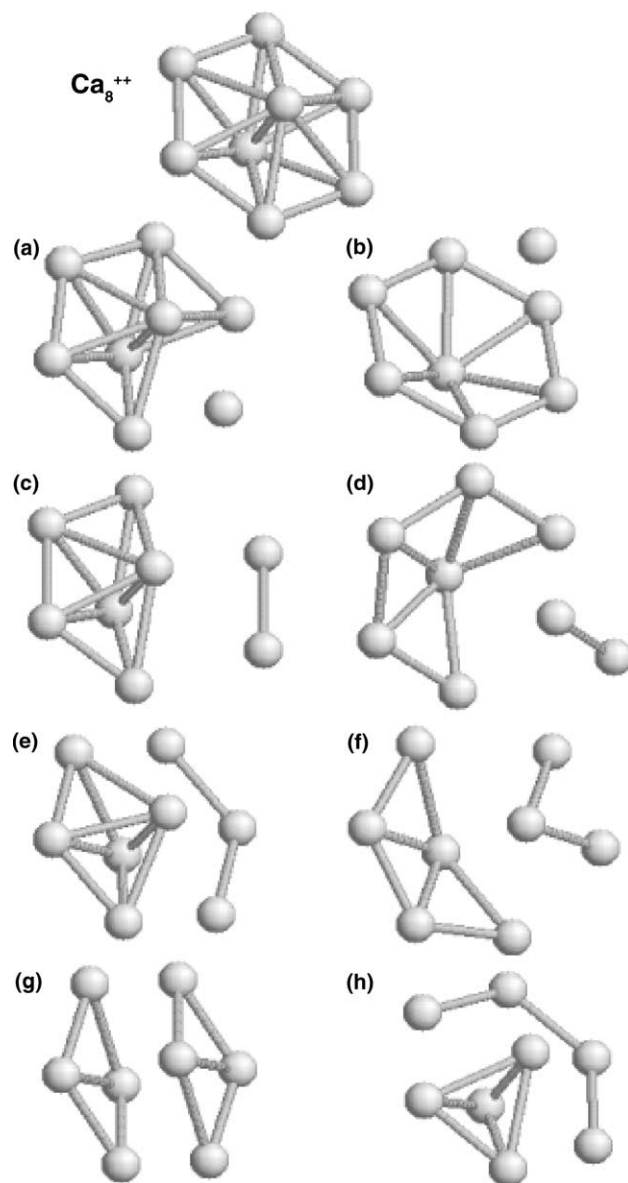

Fig. 2. Fission channels of fragmentation of Ca_8^{2+}. (a)–(h) The fission coordinate at about the position of the barrier.

barrier upper bound value of 1.24 eV should be very close to the true value. Evaporation energies are also different depending upon the way one neutral atom is pulled away from the non-equivalent sites of Ca_8^{2+} (Fig. 2a and b). The energetically favored case corresponds to Fig. 2a with barrier of 0.956 eV.

Additionally, Fig. 3 depicts the lower potential energy paths along the fission channels of 3D Ca_5^{2+} through Ca_7^{2+}. In all of them the preferred channel corresponds to $Ca_N^{2+} \rightarrow Ca_{N-1}^+ + Ca_1^+$ where the atom being removed was not an apex-atom. To reach these results we analyzed four fission channels for Ca_5^{2+} in the trigonal pyramidal structure, two channels leading to $Ca_4^+ + Ca^+$ and two other channels leading to $Ca_3^+ + Ca_2^+$. For Ca_6^{2+} in the C_{2v} structure there are a total of seven different possibilities: two channels leading
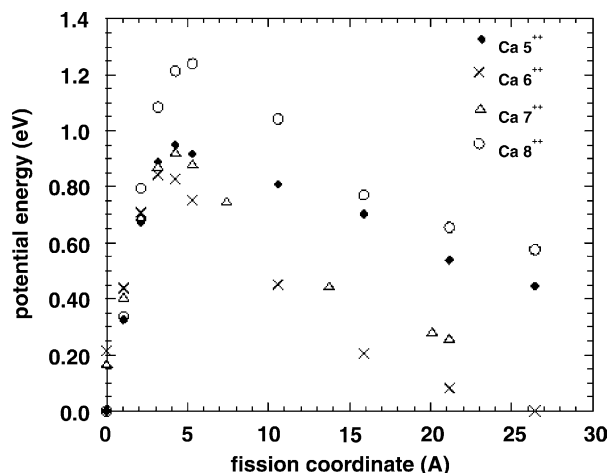
Fig. 3. The potential energy path along the preferred fission channel of fragmentation of Ca_N^{2+}: $N = 5$ (black dimond), $N = 6$ (crosses), $N = 7$ (triangles), $N = 8$ (circles). Energies and distances are referred to the bottom of the binding well.

to $Ca_5^+ + Ca^+$, three channels leading to $Ca_4^+ + Ca_2^+$, and two channels leading to $Ca_3^+ + Ca_3^+$. Similarly, there are eight different fission channels for the distorted pentagonal bipyramid Ca_7^{2+} which are: two channels for $Ca_6^+ + Ca_1^+$, and three channels for each of $Ca_5^+ + Ca_2^+$ and $Ca_4^+ + Ca_3^+$. These calculations demonstrate, and Fig. 3 illustrates, that three dimensional Ca_5^{2+} through Ca_7^{2+} fission barriers are larger than those of the linear cluster ions (Fig. 1b). Because the thermally induced transitions from 3D to linear structures of Ca_5^{2+} through Ca_7^{2+} need only 0.06 eV to occur, these ions would first become linear and then undergo fission.
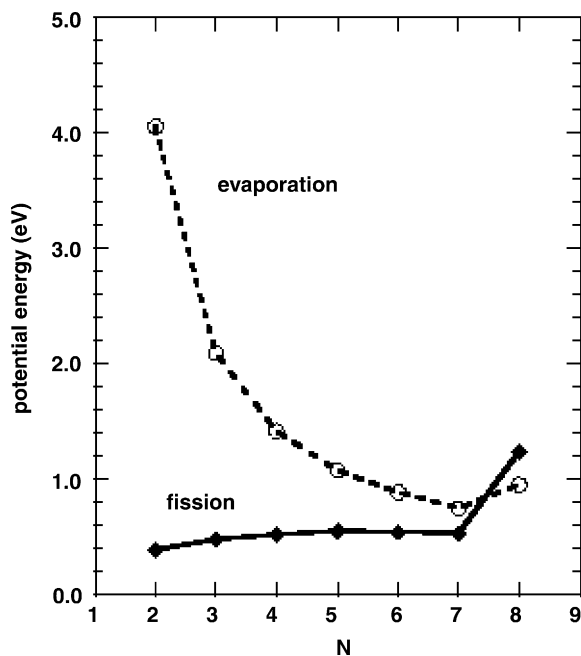
The pictorial summary of Fig. 4 compares energy barriers of the preferred fission channels of doubly ionized N-atom clusters with the evaporation energy of the same structures. Clearly Ca_7^{2+} is a turning point indicating that at this size, and below this size, the cluster ions undergo fission, but above $N = 7$ the evaporation channel is energetically more favorable. When the cluster ions fission they are linear. The appearence size is Ca_8^{2+} with a 3D-structure and a high fission barrier in agreement with experiment [5]. The small singly charged linear fragments (Ca_4^+, Ca_5^+ or Ca_6^+) resulting from fission are hot, but not enough to leave the energy well associated to that local minimum.

4. Summary

In conclusion, we have investigated all the possible fragmentation channels of Ca_N^{2+} up to $N = 8$ leading to two fragments of variable masses and charges. These fragmentation channels are classified as *fission* if the charge is the same in each fragment, and as *evaporation* if one fragment is neutral. The energy barriers for fission and evaporation were calculated and the energetically most favorable fragmentation channels were identified. Results permit the prediction that fragmentation of Ca_N^{2+} leads to fission of linear clusters below Ca_8^{2+} and to evaporation at $N = 8$ and above when the ions acquire 3D structures.

Fig. 4. Fission barriers and evaporation energies of stable Ca_N^{2+} at or below 600 K.

References

[1] O. Echt, T.D. Mark, in: H. Haberland (Ed.), Clusters of Atoms and Molecules, vol. II, Springer, Berlin, 1994, p. 183.
[2] T.P. Martin, U. Näher, H. Göhlich, T. Lange, Chem. Phys. Lett. 68 (1992) 3416.
[3] C. Bréchignac, Ph. Cahuzac, F. Carlier, M. de Frutos, Phys. Rev. Lett. 64 (1990) 2893.
[4] F. Chandezon, C. Guet, B.A. Huber, D. Jalabert, M. Manuel, E. Monnand, C. Ristori, C. Rocco, Phys. Rev. Lett. 74 (1995) 3784.
[5] M. Heinebrödt, S. Frank, N. Malinowski, F. Tast, I.M.L. Billas, T.P. Martin, Z. Phys. D 40 (1997) 334.
[6] M. Heinebrodt, N. Malinowski, F. Tast, W. Branz, I.M.L. Billas, T.P. Martin, Eur. Phys. J. D 9 (1999) 133.
[7] C. Brechignac, Ph. Cahuzac, K. Kebaili, J. Leygnier, Phys. Rev. Lett. 81 (1998) 4612.
[8] Y. Li, E. Blaisten-Barojas, Chem. Phys. Lett. 268 (1997) 331.
[9] Y. Li, E. Blaisten-Barojas, D.A. Papaconstantopoulos, Phys. Rev. B 57 (1998) 15519.
[10] D.V. Porezag, Ph.D. Thesis, Technische Universität Chemnitz-Zurickau, 1997. Basis sets are available at <http://archiv.tu-chemnitz.de/pub/1997/0025/>.
[11] M.R. Pederson, K.A. Jackson, Phys. Rev. B 41 (1990) 7453.
[12] J. Mirick, C.C. Chien, E. Blaisten-Barojas, Phys. Rev. A 63 (2001) 023202.